Dual-flow dissymmetrical low pressure steam turbine energy analysis – comparison of both turbine cylinders

Mrzljak Vedran, Lorencin Ivan, Anđelić Nikola, Car Zlatan
Faculty of Engineering, University of Rijeka, Vukovarska 58, 51000 Rijeka, Croatia
E-mail: vedran.mrzljak@riteh.hr, ilorencin@riteh.hr, nandelic@riteh.hr, zlatan.car@riteh.hr

Abstract: *In this paper is performed energy analysis of the dual-flow dissymmetrical low pressure steam turbine, which operates in a coal-fired power plant. Based on the measured operating parameters during exploitation it is calculated and presented an ideal and real power, energy losses and energy efficiencies of a whole turbine and both of its cylinders. Right cylinder of the analyzed turbine develops higher real (polytropic) and ideal (isentropic) power in comparison to left turbine cylinder. The first steam extraction of each cylinder dictates cylinder power (both ideal and real). Right cylinder has a higher energy loss and energy efficiency in comparison to left cylinder - the difference in energy loss is notable (5735.74 kW in comparison to 5447.23 kW), while the difference in energy efficiency is low, almost negligible (92.371% in comparison to 92.357%). Percentage differences between observed turbine cylinders show that left cylinder has approximately 5% lower real (polytropic) as well as ideal (isentropic) power and simultaneously approximately 5% lower energy loss.*
KEYWORDS*: DUAL-FLOW DISSYMMETRICAL STEAM TURBINE, LOW PRESSURE, TURBINE CYLINDERS PERFORMANCE COMPARISON, ENERGY ANALYSIS*

1. Introduction

Steam power plants and systems are the dominant electrical power producers worldwide [1, 2]. Along with its dominant function, steam power plants and systems can be used for various other purposes, for example as marine propulsion plants [3, 4], for simultaneous production of electrical power and heat [5], as a part of complex combined plants [6, 7], as a part of complex industry or marine plants [8-11], etc.

In the majority of steam power plants and systems, main steam turbines are composed of several cylinders, usually mounted on the same shaft [12]. Therefore, the main steam turbines are usually complex ones, while steam turbines with only one cylinder are in the most of the cases used as an auxiliary turbines [13, 14]. Steam produced in steam generators (or nuclear reactors in nuclear power plants) is in the most of the cases delivered directly to all turbines which exist in the plant [15].

Steam turbine cylinders can be single-flow or dual-flow cylinders. In dual-flow steam turbine cylinder, steam enters into the cylinder in its center and expand simultaneously through its left and right side [16]. Such dual-flow cylinders are beneficial from the viewpoint of steam axial force self-balancing. Also, such cylinders are nowadays dominantly used in nuclear power plants due to high steam mass flow rate produced in nuclear reactors [17]. Conventional steam power plants in the most of the cases use dual-flow cylinders as a low pressure cylinders (before main steam condensers).

In this paper is performed energy analysis of the dual-flow dissymmetrical low pressure steam turbine from a coal-fired power plant. Due to unequal extractions from left and right cylinder of the observed steam turbine, it was interesting to compare real and ideal power, energy efficiencies and losses of both cylinders. It is observed that, for the analyzed turbine, first steam extractions from each cylinder dictates all the obtained differences.

2. Description and characteristics of the dual-flow dissymmetrical low pressure steam turbine

The whole analyzed LPT (Low Pressure Turbine) is presented in Fig. 1. LPT is a dual-flow steam turbine, composed of two cylinders: LPC-L (Low Pressure Cylinder-Left) and LPC-R (Low Pressure Cylinder-Right). In Fig. 1 are also presented operating points required for the energy analysis. A steam mass flow rate which enters into LPT (operating point 1) is equally divided, so one its half expand through LPC-L and second half expand through LPC-R. Analyzed LPT is dissymmetrical turbine because of its extractions – in operating points 2 and 3 from the turbine cylinders are extracted different mass flow rates at different pressures.

All LPT extractions lead steam to low pressure condensate heating system [18], Fig. 1, while remaining steam mass flow rate after expansion in both cylinders (operating point 6) is delivered to steam condenser [19].

It should be highlighted that cumulative steam mass flow rate in operating points 4 and 5 is composed of two mass flow rates extracted from LPC-L and LPC-R at the same pressures for each operating point, Fig. 1. It is assumed that cumulative steam mass flow rate in operating point 4 is equally divided on the extraction from LPC-L and LPC-R. In a same manner is assumed that cumulative steam mass flow rate in operating point 5 is equally divided on the extraction from LPC-L and LPC-R.

At each cylinder outlet will be determined steam mass flow rate balances, because cumulative steam mass flow rate measured in operating point 6 is not equally divided on both LPT cylinders.

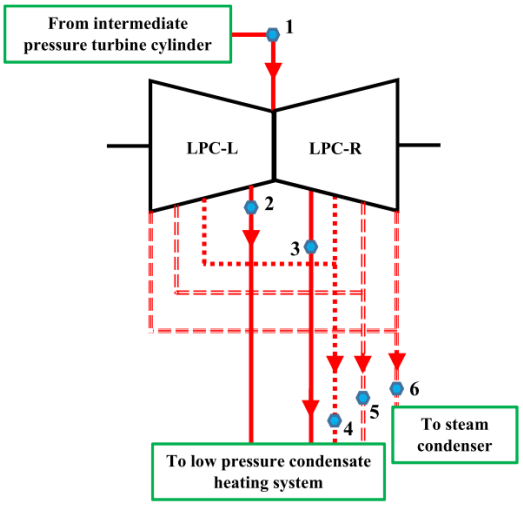

Fig. 1. *Scheme of the analyzed dual-flow dissymmetrical low pressure steam turbine along with required operating points*

Steam expansion processes (real and ideal) for both LPT cylinders are presented in h-s diagram, Fig. 2. In Fig. 2 can clearly be seen the difference between LPC-L and LPC-R real (polytropic) processes in the superheated steam area. For the LPC-L should be noted that the first extraction (operating point 2) occurs much earlier (at higher steam specific enthalpy) than the first extraction in LPC-R (operating point 3). At each extraction cylinders losses a part of the steam mass flow rate, therefore, LPC-L will earlier lose a certain amount of steam mass flow rate in comparison to LPC-R. Real (polytropic) steam expansion process of LPC-L is marked with operating points 1-2-4-5-6, while real (polytropic) LPC-R expansion process is marked with operating points 1-3-4-5-6, Fig. 2. Operating points for the real (polytropic) steam expansion processes in Fig. 2 are in accordance with operating points from Fig. 1.

Both LPT cylinders have the same ideal (isentropic) steam expansion process marked with operating point's 1-2is-3is-4is-5is-6is, Fig. 2. Ideal (isentropic) steam expansion process assume always the same steam specific entropy as at the LPT (or any cylinder) inlet, while the pressures remain the same as in the real process.

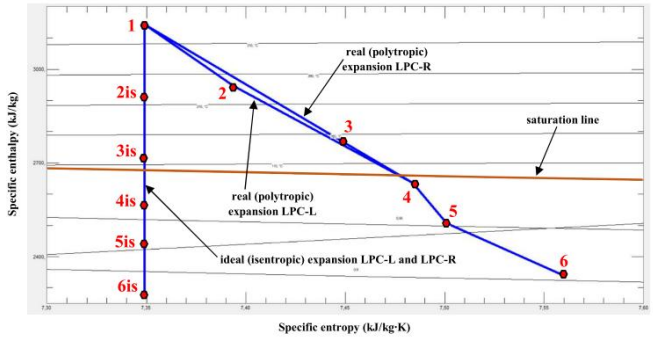

Fig. 2. *Real (polytropic) and ideal (isentropic) steam expansion processes of the LPC-L and LPC-R in h-s diagram*

3. Equations for the energy analysis

3.1. General equations and principles

In comparison to exergy analysis, which takes into consideration parameters of the ambient inside which component or system operates [20, 21], energy analysis did not take into consideration any parameter of the ambient [22, 23]. General energy balance equation, valid for any system or component, can be written as [24, 25]:

$$\dot{Q}_{\text{inlet}}+P_{\text{inlet}}+\sum \dot{E}n_{\text{inlet}} = \dot{Q}_{\text{outlet}}+P_{\text{outlet}}+\sum \dot{E}n_{\text{outlet}} \quad (1)$$

It should be highlighted that in the general energy balance equation, Eq. 1, potential and kinetic energies are disregarded [26].

In a standard operation of any system or a component, mass flow rate leakage did not occur, so mass flow rate balance is:

$$\sum \dot{m}_{\text{inlet}} = \sum \dot{m}_{\text{outlet}} \quad (2)$$

Total energy power of any fluid stream in Eq. 1, is defined according to [27] as:

$$\dot{E}n = \dot{m}\cdot h \quad (3)$$

Overall definition of any system or a component energy efficiency can be written as:

$$\eta_{\text{en}} = \frac{\text{cumulative energy outlet}}{\text{cumulative energy inlet}} \quad (4)$$

In the equations above and throughout the paper text, P is used or produced power in (kW), $\dot{Q}$ is heat transfer in (kW), $\dot{E}n$ is the total energy power of any fluid stream in (kW), $\dot{m}$ is the fluid mass flow rate in (kg/s), h is fluid specific enthalpy in (kJ/kg) and η is efficiency.

3.2. Equations for the energy analysis of low pressure steam turbine and both of its cylinders

Equations for the energy analysis of the whole LPT and both of its cylinders (LPC-L and LPC-R) are based on the operating points presented in Fig. 1 and Fig. 2.

LPT left cylinder (LPC-L)

- Mass flow rate balance:

$$\dot{m}_{6,\text{Left}} = \frac{\dot{m}_1}{2} - \dot{m}_2 - \frac{\dot{m}_4}{2} - \frac{\dot{m}_5}{2} \quad (5)$$

- Real (polytropic) power:

$$P_{\text{re,LPC-L}} = \frac{\dot{m}_1}{2}\cdot\left(h_1-h_2\right)+\left(\frac{\dot{m}_1}{2}-\dot{m}_2\right)\cdot\left(h_2-h_4\right)+\left(\frac{\dot{m}_1}{2}-\dot{m}_2-\frac{\dot{m}_4}{2}\right)\cdot\left(h_4-h_5\right)+\left(\frac{\dot{m}_1}{2}-\dot{m}_2-\frac{\dot{m}_4}{2}-\frac{\dot{m}_5}{2}\right)\cdot\left(h_5-h_6\right) \quad (6)$$

- Ideal (isentropic) power:

$$P_{\text{id,LPC-L}} = \frac{\dot{m}_1}{2}\cdot\left(h_1-h_{2\text{is}}\right)+\left(\frac{\dot{m}_1}{2}-\dot{m}_2\right)\cdot\left(h_{2\text{is}}-h_{4\text{is}}\right)+\left(\frac{\dot{m}_1}{2}-\dot{m}_2-\frac{\dot{m}_4}{2}\right)\cdot h_{4\text{is}}-h_{5\text{is}} + \left(\frac{\dot{m}_1}{2}-\dot{m}_2-\frac{\dot{m}_4}{2}-\frac{\dot{m}_5}{2}\right)\cdot h_{5\text{is}}-h_{6\text{is}} \quad (7)$$

- Energy power loss:

$$\dot{E}n_{\text{Loss,LPC-L}} = P_{\text{id,LPC-L}} - P_{\text{re,LPC-L}} \quad (8)$$

- Energy efficiency:

$$\eta_{\text{en,LPC-L}} = \frac{P_{\text{re,LPC-L}}}{P_{\text{id,LPC-L}}} \quad (9)$$

LPT right cylinder (LPC-R)

- Mass flow rate balance:

$$\dot{m}_{6,\text{Right}} = \frac{\dot{m}_1}{2} - \dot{m}_3 - \frac{\dot{m}_4}{2} - \frac{\dot{m}_5}{2} \quad (10)$$

Energy analysis of LPC-R is performed with a same equations as for LPC-L (from Eq. 6 to Eq. 9), by using this modifications:

- In all the equations from Eq. 6 to Eq. 9, index LPC-L should be changed with LPC-R,
- In Eq. 6, $\dot{m}_2$ should be replaced with $\dot{m}_3$ and h_2 should be replaced with h_3,
- In Eq. 7, $\dot{m}_2$ should be replaced with $\dot{m}_3$ and $h_{2\text{is}}$ should be replaced with $h_{3\text{is}}$.

Whole LPT (WLPT)

- Mass flow rate balance:

$$\dot{m}_6 = \dot{m}_{6,\text{Left}} + \dot{m}_{6,\text{Right}} \quad (11)$$

- Real (polytropic) power:

$$P_{\text{re,WLPT}} = P_{\text{re,LPC-L}} + P_{\text{re,LPC-R}} \quad (12)$$

- Ideal (isentropic) power:

$$P_{\text{id,WLPT}} = P_{\text{id,LPC-L}} + P_{\text{id,LPC-R}} \quad (13)$$

- Energy power loss:

$$\dot{E}n_{\text{Loss,WLPT}} = P_{\text{id,WLPT}} - P_{\text{re,WLPT}} \quad (14)$$

- Energy efficiency:

$$\eta_{\text{en,WLPT}} = \frac{P_{\text{re,WLPT}}}{P_{\text{id,WLPT}}} \quad (15)$$

Comparison of LPC-L and LPC-R

Comparison of both LPT cylinders is performed as a percentage difference of calculated values:

$$\text{Difference (\%)} = 100 - \frac{\text{calculated value for LPC-L}}{\text{calculated value for LPC-R}}\cdot 100 \quad (16)$$

4. Steam operating parameters

For the analyzed LPT, steam operating parameters in each operating point of Fig. 1 were found in [28] and presented in Table 1. According to the steam operating parameters from Table 1 are calculated all the other operating parameters in each operating point of Fig. 1 required for the analysis.

Table 1. *Steam parameters in each operating point of Fig. 1 [28]*

O.P.*	Mass flow rate (kg/s)	Pressure (bar)	Specific enthalpy (kJ/kg)
1	183.38	8.600	3144.39
2	10.39	3.600	2946.62
3	6.43	1.300	2758.30
4	6.96	0.600	2635.89
5	8.06	0.250	2506.11
6	151.56	0.065	2339.02

* O.P. = Operating Point (according to Fig. 1)

From known steam pressure and specific enthalpy in each operating point of Fig. 1 (Table 1) are calculated steam temperature, steam specific entropy and steam quality by using NIST-REFPROP 9.0 software [29] and presented in Table 2.

Table 2. *Calculated steam operating parameters in each operating point of Fig. 1*

O.P.*	Temperature (°C)	Specific entropy (kJ/kg/K)	Steam quality
1	342.14	7.3490	Superheated
2	240.61	7.3939	Superheated
3	142.00	7.4512	Superheated
4	85.93	7.4839	0.993
5	64.96	7.5009	0.953
6	37.63	7.5598	0.905

* O.P. = Operating Point (according to Fig. 1)

Ideal (isentropic) steam expansion process assumes always the same steam specific entropy as at the LPT inlet (pressures during such expansion remains the same as in the real expansion process). For LPC-L and LPC-R ideal expansion process is the same, Figure 2. Isentropic specific enthalpies, required for the calculation of ideal (isentropic) power of the LPT and both of its cylinders, are also calculated by using NIST-REFPROP 9.0 software [29] (according to Fig. 2) and presented in Table 3.

Table 3. *Calculated steam operating parameters for the ideal (isentropic) expansion*

O.P.*	Pressure (bar)	Specific entropy (kJ/kg/K)	Isentropic specific enthalpy (kJ/kg)
1	8.600	7.3490	3144.39
2is	3.600	7.3490	2923.80
3is	1.300	7.3490	2716.90
4is	0.600	7.3490	2587.50
5is	0.250	7.3490	2454.80
6is	0.065	7.3490	2273.50

* O.P. = Operating Point (according to Fig. 2)

5. Results and discussion

As noted in the description of Fig. 2 and in Table 1, LPC-L has first extraction in operating point 2 at the higher pressure in comparison to first extraction from LPC-R (operating point 3), Fig. 1. This element results with a fact that the LPC-L will earlier lose a certain amount of steam mass flow rate and after the first extraction throughout LPC-L will expand lower steam mass flow rate in comparison to LPC-R. The result of such extractions in both of the cylinders is that the LPC-R develop higher real (polytropic) and ideal (isentropic) power in comparison to LPC-L. Real and ideal LPC-L power are equal to 65828.14 kW and 71275.36 kW, respectively, while the real and ideal LPC-R power are equal to 69444.86 kW and 75180.61 kW, respectively, Fig. 3.

The whole LPT develops real (polytropic) power equal to 135273 kW, while ideal (isentropic) power of the whole LPT is equal to 146455.97 kW, Fig. 3.

From the considerations above can be concluded that the first steam extraction of each LPT cylinder dictates cylinder power (both ideal and real). The lower pressure and lower quantity of extracted steam mass flow rate in the first extraction of any cylinder will lead to higher power.

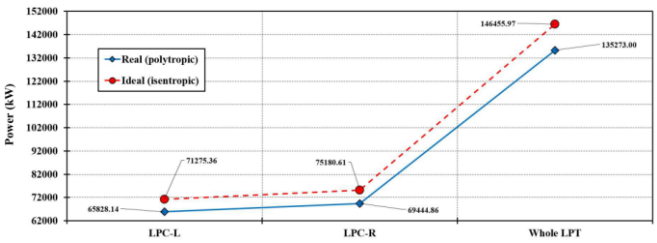

Fig. 3. *Real (polytropic) and ideal (isentropic) power of LPC-L and LPC-R as well as of the whole observed LPT*

A comparison of both observed cylinders shows that the LPC-R has higher energy loss and higher energy efficiency. The difference in energy loss between LPC-L and LPC-R is notable (5447.23 kW in comparison to 5735.74 kW), while the difference in energy efficiency between two observed cylinders is low, almost negligible (92.357% in comparison to 92.371%), Fig. 4.

Energy loss of the whole observed LPT is equal to 11182.97 kW and its energy efficiency equals 92.364%, Fig. 4. The final comparison in observed operating parameters between LPC-L and LPC-R will be presented in Fig. 5.

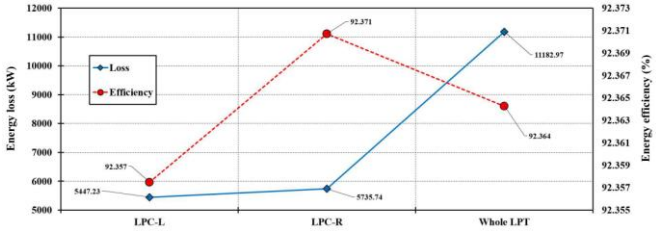

Fig. 4. *Energy loss and energy efficiency of LPC-L and LPC-R as well as of the whole LPT*

As can be seen from Fig. 5, comparison of differences between LPC-L and LPC-R shows that the LPC-L has approximately 5% lower real (polytropic) and ideal (isentropic) power as well as approximately 5% lower energy loss in comparison to LPC-R. The percentage difference in energy efficiency between two observed cylinders is almost negligible.

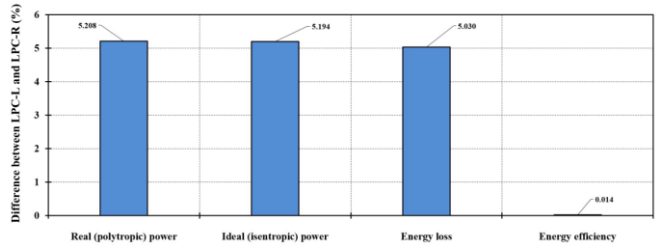

Fig. 5. *Percentage difference in calculated power, energy loss and energy efficiency between LPC-L and LPC-R*

Further research of the analyzed dual-flow dissymmetrical steam turbine and comparison of the obtained results with other dual-flow dissymmetrical steam turbines will be based on the results of energy and exergy analyses (turbine and both cylinders power, efficiencies and losses). The intention will be to create a sufficient dataset on which will be applied artificial intelligence techniques and methods already developed by our research team [30-35]. As a final result, the goal will be to obtain accurate and precise algorithm for a fast prediction of differences between cylinders in any dual-flow dissymmetrical steam turbine.

6. Conclusions

This paper presents an energy analysis of the dual-flow dissymmetrical low pressure steam turbine. Unequal extractions from left and right cylinder of the observed steam turbine makes various differences between observed cylinders. Based on the measured operating parameters from exploitation it is calculated ideal and real power, energy efficiency and energy loss for both cylinders and a whole turbine. The main conclusions obtained in this analysis are:

- The first steam extraction of each LPT cylinder dictates cylinder power (both ideal and real). The lower pressure and lower quantity of extracted steam mass flow rate in the first extraction of any cylinder will lead to higher power.
- LPC-R develops higher real (polytropic) and ideal (isentropic) power in comparison to LPC-L. The real and ideal power of LPC-L are equal to 65828.14 kW and 71275.36 kW, while the real and ideal power of LPC-R are equal to 69444.86 kW and 75180.61 kW, respectively.

- LPC-R has a higher energy loss and higher energy efficiency in comparison to LPC-L. The difference in energy loss is notable (5735.74 kW in comparison to 5447.23 kW), while the difference in energy efficiency is low, almost negligible (92.371% in comparison to 92.357%).
- Comparison of differences between LPC-L and LPC-R shows that the LPC-L has approximately 5% lower real (polytropic) and ideal (isentropic) power as well as approximately 5% lower energy loss. The percentage difference in energy efficiency between two observed cylinders is almost negligible.

7. Acknowledgment

This research has been supported by the Croatian Science Foundation under the project IP-2018-01-3739, CEEPUS network CIII-HR-0108, European Regional Development Fund under the grant KK.01.1.1.01.0009 (DATACROSS), project CEKOM under the grant KK.01.2.2.03.0004, CEI project "COVIDAi" (305.6019-20), University of Rijeka scientific grant uniri-tehnic-18-275-1447 and University of Rijeka scientific grant uniri-tehnic-18-18-1146.

8. References

[1] Erdem, H. H., Akkaya, A. V., Cetin, B., Dagdas, A., Sevilgen, S. H., Sahin, B., ... & Atas, S. (2009). *Comparative energetic and exergetic performance analyses for coal-fired thermal power plants in Turkey*. International Journal of Thermal Sciences, 48(11), 2179-2186. (doi:10.1016/j.ijthermalsci.2009.03.007)

[2] Blažević, S., Mrzljak, V., Anđelić, N., & Car, Z. (2019). *Comparison of energy flow stream and isentropic method for steam turbine energy analysis*. Acta Polytechnica, 59(2), 109-125. (doi:10.14311/AP.2019.59.0109)

[3] Koroglu, T., & Sogut, O. S. (2018). *Conventional and advanced exergy analyses of a marine steam power plant*. Energy, 163, 392-403. (doi:10.1016/j.energy.2018.08.119)

[4] Mrzljak, V., & Poljak, I. (2019). *Energy Analysis of Main Propulsion Steam Turbine from Conventional LNG Carrier at Three Different Loads*. NAŠE MORE: znanstveno-stručni časopis za more i pomorstvo, 66(1), 10-18. (doi:10.17818/NM/2019/1.2)

[5] Burin, E. K., Vogel, T., Multhaupt, S., Thelen, A., Oeljeklaus, G., Görner, K., & Bazzo, E. (2016). *Thermodynamic and economic evaluation of a solar aided sugarcane bagasse cogeneration power plant*. Energy, 117, 416-428. (doi:10.1016/j.energy.2016.06.071)

[6] Ersayin, E., & Ozgener, L. (2015). *Performance analysis of combined cycle power plants: A case study*. Renewable and Sustainable Energy Reviews, 43, 832-842. (doi:10.1016/j.rser.2014.11.082)

[7] Lorencin, I., Anđelić, N., Mrzljak, V., & Car, Z. (2019). *Genetic Algorithm Approach to Design of Multi-Layer Perceptron for Combined Cycle Power Plant Electrical Power Output Estimation*. Energies, 12(22), 4352. (doi:10.3390/en12224352)

[8] Hafdhi, F., Khir, T., Yahyia, A. B., & Brahim, A. B. (2015). *Energetic and exergetic analysis of a steam turbine power plant in an existing phosphoric acid factory*. Energy Conversion and Management, 106, 1230-1241. (doi:10.1016/j.enconman.2015.10.044)

[9] Mrzljak, V., Poljak, I., & Medica-Viola, V. (2017). *Dual fuel consumption and efficiency of marine steam generators for the propulsion of LNG carrier*. Applied Thermal Engineering, 119, 331-346. (doi:10.1016/j.applthermaleng.2017.03.078)

[10] Behrendt, C., & Stoyanov, R. (2018). *Operational Characteristic of Selected Marine Turbounits Powered by Steam from Auxiliary Oil-Fired Boilers*. New Trends in Production Engineering, 1(1), 495-501. (doi:10.2478/ntpe-2018-0061)

[11] Medica-Viola, V., Mrzljak, V., Anđelić, N., & Jelić, M. (2020). *Analysis of Low-Power Steam Turbine With One Extraction for Marine Applications*. NAŠE MORE: znanstveni časopis za more i pomorstvo, 67(2), 87-95. (doi:10.17818/NM/2020/2.1)

[12] Adibhatla, S., & Kaushik, S. C. (2014). *Energy and exergy analysis of a super critical thermal power plant at various load conditions under constant and pure sliding pressure operation*. Applied thermal engineering, 73(1), 51-65. (doi:10.1016/j.applthermaleng.2014.07.030)

[13] Mrzljak, V. (2018). *Low power steam turbine energy efficiency and losses during the developed power variation*. Tehnički glasnik, 12(3), 174-180. (doi:10.31803/tg-20180201002943)

[14] Mrzljak, V., Senčić, T., & Žarković, B. (2018). *Turbogenerator steam turbine variation in developed power: Analysis of exergy efficiency and exergy destruction change*. Modelling and Simulation in Engineering, 2018. (doi:10.1155/2018/2945325)

[15] Mrzljak, V., Prpić-Oršić, J., & Senčić, T. (2018). *Change in steam generators main and auxiliary energy flow streams during the load increase of LNG carrier steam propulsion system*. Pomorstvo, 32(1), 121-131. (doi:10.31217/p.32.1.15)

[16] Ahmadi, G. R., & Toghraie, D. (2016). *Energy and exergy analysis of Montazeri steam power plant in Iran*. Renewable and Sustainable Energy Reviews, 56, 454-463. (doi:10.1016/j.rser.2015.11.074)

[17] Wang, C., Yan, C., Wang, J., Tian, C., & Yu, S. (2017). *Parametric optimization of steam cycle in PWR nuclear power plant using improved genetic-simplex algorithm*. Applied Thermal Engineering, 125, 830-845. (doi:10.1016/j.applthermaleng.2017.07.045)

[18] Mrzljak, V., Poljak, I., & Medica-Viola, V. (2016). *Efficiency and losses analysis of low-pressure feed water heater in steam propulsion system during ship maneuvering period*. Pomorstvo, 30(2), 133-140. (doi:10.31217/p.30.2.6)

[19] Škopac, L., Medica-Viola, V., & Mrzljak, V. (2020). *Selection Maps of Explicit Colebrook Approximations according to Calculation Time and Precision*. Heat Transfer Engineering, 1-15. (doi:10.1080/01457632.2020.1744248)

[20] Lorencin, I., Anđelić, N., Mrzljak, V., & Car, Z. (2019). *Exergy analysis of marine steam turbine labyrinth (gland) seals*. Pomorstvo, 33(1), 76-83. (doi:10.31217/p.33.1.8)

[21] Szargut, J. (2005). *Exergy method: technical and ecological applications* (Vol. 18). WIT press.

[22] Baldi, F., Ahlgren, F., Nguyen, T. V., Thern, M., & Andersson, K. (2018). *Energy and exergy analysis of a cruise ship*. Energies, 11(10), 2508. (doi:10.3390/en11102508)

[23] Mrzljak, V., Prpić-Oršić, J., & Poljak, I. (2018). *Energy Power Losses and Efficiency of Low Power Steam Turbine for the Main Feed Water Pump Drive in the Marine Steam Propulsion System*. Pomorski zbornik, 54(1), 37-51. (doi:10.18048/2018.54.03)

[24] Medica-Viola, V., Baressi Šegota, S., Mrzljak, V., & Štifanić, D. (2020). *Comparison of conventional and heat balance based energy analyses of steam turbine*. Pomorstvo, 34(1), 74-85. (doi:10.31217/p.34.1.9)

[25] Aljundi, I. H. (2009). *Energy and exergy analysis of a steam power plant in Jordan*. Applied thermal engineering, 29(2-3), 324-328. (doi:10.1016/j.applthermaleng.2008.02.029)

[26] Mrzljak, V., Blecich, P., Anđelić, N., & Lorencin, I. (2019). *Energy and Exergy Analyses of Forced Draft Fan for Marine Steam Propulsion System during Load Change*. Journal of Marine Science and Engineering, 7(11), 381. (doi:10.3390/jmse7110381)

[27] Kanoğlu, M., Çengel, Y. A., & Dinçer, İ. (2012). *Efficiency evaluation of energy systems*. Springer Science & Business Media.

[28] Zhang, C., Wang, Y., Zheng, C., & Lou, X. (2006). *Exergy cost analysis of a coal fired power plant based on structural theory of thermoeconomics*. Energy Conversion and Management, 47(7-8), 817-843. (doi:10.1016/j.enconman.2005.06.014)

[29] Lemmon, E. W., Huber, M. L., & McLinden, M. O. (2010). *NIST Standard Reference Database 23, Reference Fluid Thermodynamic and Transport Properties (REFPROP)*, version 9.0, National Institute of Standards and Technology. R1234yf. fld file dated December, 22, 2010.

[30] Car, Z., Baressi Šegota, S., Anđelić, N., Lorencin, I., & Mrzljak, V. (2020). *Modeling the Spread of COVID-19 Infection Using a Multilayer Perceptron*. Computational and Mathematical Methods in Medicine, 2020. (doi:10.1155/2020/5714714)

[31] Lorencin, I., Anđelić, N., Mrzljak, V., & Car, Z. (2019). *Marine Objects Recognition Using Convolutional Neural Networks*. NAŠE MORE: znanstveno-stručni časopis za more i pomorstvo, 66(3), 112-119. (doi:10.17818/NM/2019/3.3)

[32] Baressi Šegota, S., Lorencin, I., Ohkura, K., & Car, Z. (2019). *On the Traveling Salesman Problem in Nautical Environments: an Evolutionary Computing Approach to Optimization of Tourist Route Paths in Medulin, Croatia*. Pomorski zbornik, 57(1), 71-87. (doi:10.18048/2019.57.05)

[33] Lorencin, I., Anđelić, N., Mrzljak, V., & Car, Z. (2019). *Multilayer Perceptron approach to Condition-Based Maintenance of Marine CODLAG Propulsion System Components*. Pomorstvo, 33(2), 181-190. (doi:10.31217/p.33.2.8)

[34] Lorencin, I., Anđelić, N., Španjol, J., & Car, Z. (2020). *Using multi-layer perceptron with Laplacian edge detector for bladder cancer diagnosis*. Artificial Intelligence in Medicine, 102, 101746. (doi:10.1016/j.artmed.2019.101746)

[35] Baressi Šegota, S., Lorencin, I., Musulin, J., Štifanić, D., & Car, Z. (2020). *Frigate Speed Estimation Using CODLAG Propulsion System Parameters and Multilayer Perceptron*. NAŠE MORE: znanstveni časopis za more i pomorstvo, 67(2), 117-125. (doi:10.17818/NM/2020/2.4)